

1
2
3
4
5
6
7

8 **Feedback-dependent Generalization**

9 Jordan A. Taylor¹, Laura L. Hieber², Richard B. Ivry^{2,3}

10 ¹Department of Psychology, Princeton University

11 ²Department of Psychology, University of California, Berkeley

12 ³Helen Wills Neuroscience Institute, University of California, Berkeley

13
14
15
16

17 Corresponding Author:

18 Jordan A. Taylor

19 Department of Psychology

20 Princeton University

21 3-S-13 Green Hall

22 Princeton, NJ 08544

23 Phone: (609) 258-4648

24 Fax: (609) 258-1113

25 jordanat@princeton.edu

26

27 Manuscript Details:

28 Words Count: 9207

29 Number of Pages: 34 of text; 45 with figures.

30 Number of Figures: 11

31 Number of Tables: 2

32

33

34 **Abstract**
35
36 Generalization provides a window into the representational changes that occur
37 during motor learning. Neural network models have been integral in revealing how the
38 neural representation constrains the extent of generalization. Specifically, two key
39 features are thought to define the pattern of generalization. First, generalization is
40 constrained by the properties of the underlying neural units; with directionally-tuned
41 units, the extent of generalization is limited by the width of the tuning functions. Second,
42 error signals are used to update a sensorimotor map to align the desired and actual
43 output, with a gradient-descent learning rule ensuring that the error produces changes
44 in those units responsible for the error. In prior studies, task-specific effects in
45 generalization have been attributed to differences in neural tuning functions. Here we
46 ask if differences in generalization functions may arise from task-specific error signals.
47 We systematically varied visual error information in a visuomotor adaptation task, and
48 found that this manipulation led to qualitative differences in generalization. A neural
49 network model suggests that these differences are the result of error feedback
50 processing operating on a homogenous and invariant set of tuning functions.
51 Consistent with novel predictions derived from the model, increasing the number of
52 training directions led to specific distortions of the generalization function. Taken
53 together, the behavioral and modeling results offer a parsimonious account of
54 generalization that is based on the utilization of feedback information to update a
55 sensorimotor map with stable tuning functions.

56
57
58 **Introduction**
59
60 Generalization has been used as a probe on the representational changes that
61 occur during learning (Thoroughman and Shadmehr 2000; Poggio and Bizzì 2004). A
62 common method to study generalization is to employ a visuomotor perturbation that
63 introduces errors between a desired movement and the actual movement. Participants
64 are trained with this perturbation in one movement direction or in a limited region of the
65 workspace, and then tested with movements in other directions (Ghahramani, Wolpert
66 et al. 1996; Pine, Krakauer et al. 1996; Krakauer, Pine et al. 2000). How the system

67 generalizes from a limited training set can provide insight into computational principles
68 underlying sensorimotor learning and control (Poggio and Bizzi 2004), such as relating
69 the pattern of generalization to the neural tuning properties (Donchin, Francis et al.
70 2003; Poggio and Bizzi 2004; Thoroughman and Taylor 2005).

71 A range of visuomotor perturbations have been employed in studies of
72 generalization. Somewhat surprisingly, the results have failed to provide a consistent
73 picture of generalization. Visuomotor rotations in which an angular displacement is
74 imposed between the position of the unseen hand and a visual cursor results in rather
75 narrow generalization (Pine, Krakauer et al. 1996; Krakauer, Pine et al. 2000).
76 Generalization is prominent for directions similar to the trained direction, but falls off
77 sharply as the probed directions differ from the trained direction (Pine, Krakauer et al.
78 1996; Krakauer, Pine et al. 2000; Tanaka, Sejnowski et al. 2009). Visuomotor gain
79 adaptation, in which the amplitude between hand movement and cursor displacement is
80 altered, also produces maximal generalization near the direction of training, but exhibits
81 considerable generalization for all directions of movement (Krakauer, Pine et al. 2000;
82 Vindras and Viviani 2002; Pearson, Krakauer et al. 2010). Similarly, linear shifts of the
83 visual input, the type of perturbation created by prism glasses, generalizes relatively
84 broadly across the workspace (Ghahramani, Wolpert et al. 1996). Dynamic
85 perturbations such as those employed in studies using force fields environments, have
86 also been used to study generalization. The results from this work indicate that the
87 pattern of generalization is dependent on the complexity of the perturbation
88 (Thoroughman and Shadmehr 2000; Donchin, Francis et al. 2003; Thoroughman and
89 Taylor 2005).

90 While certain features of generalization functions are similar across these studies
91 (e.g., maximal generalization for movements most similar to the training set), the subtle
92 differences have been the focus of considerable debate given their potential to reveal
93 the representational changes that occur during sensorimotor learning. Two key features
94 are thought to define the form of generalization. First, generalization will be constrained
95 by the underlying units that control the movements. For example, if the units are
96 directionally-tuned neurons, generalization is constrained by the width of the tuning
97 functions (Thoroughman and Shadmehr 2000). Second, errors are used to update the

98 sensorimotor map, altering the weights between the tuned units and desired directions
99 of movement (Pouget and Snyder 2000). Learning algorithms combine these two
100 features to ensure that the error only modifies those units which were responsible for
101 the error. As such, if the underlying units represent movement space broadly,
102 generalization will be broad because many units are affected by the error signal
103 (Thoroughman and Shadmehr 2000). In contrast, if the units represent space narrowly,
104 then generalization will be limited given that units tuned to distant directions are
105 unaffected by the error. Thus, patterns of generalization have been used to identify
106 computational properties of the motor control system (Ghahramani, Wolpert et al. 1996;
107 Pouget and Snyder 2000; Thoroughman and Shadmehr 2000; Poggio and Bizzi 2004).

108 As described above, generalization studies have been exploited to explore the
109 tuning properties of motor control elements (Thoroughman and Shadmehr 2000). For
110 example, Thoroughman and Taylor (2005) trained participants to move in force field
111 environments with varying degrees of dynamical complexity. While learning was
112 reasonably similar across conditions, the generalization functions were quite different.
113 To account for these differences, two hypotheses were suggested. One centered on
114 the idea that there exists a heterogeneous population of tuning functions with a range of
115 widths; by this account, the relevant set of tuning functions for learning will vary with
116 task complexity. The second hypothesis centered on the idea that the width of the
117 tuning functions is altered with training, and that the extent of these changes will vary
118 with task complexity. While experimental studies testing these hypotheses have not
119 been reported, both hypotheses necessitate that the tuning function of the neural units
120 must be different to learn different environmental complexities.

121 A few studies have asked how error signals may contribute to task-dependent
122 effects on generalization. Depending on the form of a visuomotor perturbation (e.g.,
123 rotational or translational), generalization can either be expressed in a Cartesian
124 reference frame or rotational (Ghahramani, Wolpert et al. 1996; Krakauer, Pine et al.
125 2000). Moreover, the strength of generalization is influenced by the availability of error
126 information: Adaptation (Rapp and Heuer 2011) and generalization are stronger when
127 feedback is continuously available during the reach compared to when it is provided
128 only at the end of movement (Hinder, Tresilian et al. 2008; Shabbott and Sainburg

129 2010). Although the consequences of these error manipulations have not been
130 examined in a formal manner these results suggest that task-dependent differences in
131 generalization may reflect variation in the availability of error information for adapting
132 the sensorimotor system. Specifically, a change in error information may influence
133 generalization because more states are subject to error-based modification during
134 training.

135 The current study was designed to provide a systematic analysis of the influence
136 of error information on generalization. In the main experiment, participants were trained
137 on a visuomotor rotation task, with the training phase limited to a single direction of
138 movement, followed by generalization to untrained, distant locations. Between groups,
139 we manipulated the form of the visual feedback, providing either endpoint or on-line
140 feedback, and within the latter, varying whether or not the movement had to terminate in
141 the target location. While the groups displayed similar learning curves during the
142 training period, they exhibited strikingly different generalization patterns. Building on
143 previous work (Thoroughman and Shadmehr 2000; Thoroughman and Taylor 2005;
144 Tanaka, Sejnowski et al. 2009; Pearson, Krakauer et al. 2010), we employed a radial
145 basis function network to simulate the patterns of generalization. We show that
146 qualitatively different patterns of generalization can be produced in such a network due
147 to variation in the error signal, even if the underlying tuning functions remain invariant.
148 A second experiment was conducted in which we extended the range of training
149 directions to test a novel prediction derived from the model.

150

151 **Materials and Methods**

152

153 *Participants and Experimental Apparatus*

154 Sixty young adults (35 females/25 males, age 22 ± 7 years) were recruited from the
155 research participation pool maintained by the Department of Psychology at the
156 University of California, Berkeley. All participants were right-handed, verified with the
157 Edinburgh handedness inventory (Oldfield 1971), and received class credit. The
158 experimental protocol was approved by the University of California's IRB.

159 Participants made center-out, horizontal reaching movements to visually displayed
160 targets, sliding their right hand across a digitizing tablet while holding onto a digitizing

161 pen (Intuos 3, Wacom, Vancouver, WA, USA). Movement trajectories were sampled
162 at 100 Hz. The stimuli and feedback cursor were displayed on a 15-inch, 1280x1024
163 pixel resolution LCD computer monitor (Dell, Dallas, TX, USA) horizontally mounted
164 25.4 cm above the table. Since the monitor occluded vision of the hand, visual feedback
165 was in the form of a small circular cursor (3.5 mm).

166

167 *Experiment 1*

168 Forty participants were assigned to one of four experimental groups (Figure 1),
169 with 10 participants per group. For all groups, the trial started with the participant
170 moving his or her hand such that the feedback cursor was positioned in a starting circle
171 (5 mm diameter). After 1 s at this position, a green target (7 mm diameter dot)
172 appeared on a blue ring (7 cm in radial distance from the starting circle. The target
173 could appear in one of 8 locations (0°, 45°, 90°, 135°, 180°, -135°, -90°, -45°). The
174 participants were instructed to make a fast reaching movement to the target.

175 For the endpoint-feedback group (ENDPOINT group), participants only received
176 endpoint feedback of the movement (knowledge of results). These participants were
177 instructed to make a fast reaching movement, attempting to slice through the target.
178 The feedback cursor disappeared when the participant's hand exited the starting circle.
179 When the participant's hand had moved 7 cm, a red cursor (3.5 mm) appeared at the
180 corresponding position (veridical or rotated) on the blue ring and remained visible for 1
181 s. For the online-feedback group (ONLINE group), feedback of hand position was
182 provided during the entire outbound portion of the movement. When the radial
183 amplitude reached 7 cm, the white cursor changed to red and remained positioned on
184 the blue ring for 1 s (as with the ENDPOINT group). Participants in the ENDPOINT and
185 ONLINE groups, were instructed that the goal was to have the red feedback cursor be
186 positioned as close to the target as possible. In contrast, participants in the corrective-
187 feedback group (CORRECTIVE group) received online feedback and were required to
188 bring the white cursor within the target circle to end the trial. When any part of the
189 cursor overlapped the target, the feedback color changed to red and remained fixed in
190 place for 1 s.

191 Participants in all three groups were trained to reach the blue ring within 300-500

192 ms. If this criterion was met, a pleasant “ding” sound was played; otherwise an
193 unpleasant “buzz” sound was played. In addition, if the movement time criterion was
194 met and any part of the feedback cursor overlapped the target, the participant received
195 1 point. Note that CORRECTIVE participants always had to hit the target; thus, their
196 bonus was solely dependent on the temporal criterion. The points were tallied
197 throughout the experiment, with the sum displayed at the end of each block.

198 Following the 1 s endpoint feedback delay, participants in the ENDPOINT,
199 ONLINE, and CORRECTIVE groups were required to reposition the hand in the starting
200 circle. The participant was guided to the starting position by a white ring with diameter
201 equal to the distance of the hand from the starting position. By moving towards the
202 starting circle, this ring became progressively smaller. When the hand was within 1 cm
203 of the starting circle, the ring was transformed into the white feedback cursor, allowing
204 the participant to position the hand within the starting circle.

205 Participants in the return-feedback group (RETURN group) had continuous online
206 feedback of the cursor during both the out and back phases of the movement. They
207 were instructed to reach the target within 300-500 ms, with the feedback cursor
208 changing from white to red when it overlapped any part of the target. The feedback
209 cursor remained fixed at this position for 1 s, before changing back to white.
210 Participants were instructed to keep their hand still during the 1 s feedback interval. If
211 the participant moved more than 1 cm from the terminal position, a double buzz sound
212 was played to remind the participant that they should remain still during the feedback
213 interval. Once the feedback cursor turned white, the participant was instructed to return
214 to the starting circle. There was no temporal criterion for the return movement, but
215 online feedback was available at all times.

216 All participants made a total of 266 movements, divided into a series of blocks
217 (Figure 1). The groups were initially trained with their assigned feedback format for 64
218 baseline trials, with each of the eight target locations presented eight times. Feedback
219 was veridical during this phase, allowing the participants to become accustomed to the
220 reaching task and learn the desired movement speed. Participants then made another
221 32 baseline movements, four to each target. On half of the trials, feedback was
222 presented. On the other half of the trials, the feedback went blank at the start of the

223 movement. Participants were not informed if a trial included feedback or not, only
224 discovering this once the movement started. On no-feedback trials, the participants
225 were instructed to just reach through the visible blue ring, attempting to maintain their
226 adopted movement velocity. For all groups, the contracting white ring was used to
227 guide the hand back to the starting position after each no-feedback trial. This block was
228 included to provide the participants with experience at moving in the absence of
229 feedback.

230 The two baseline blocks were followed by a 40-trial rotation block. For this block,
231 all of the reaches were to a single “training” location at 0°. Feedback of hand position
232 (either on-line or endpoint, depending on the group) was rotated 30° counterclockwise
233 (CCW). The rotation block was followed by a test block in which reaches to the training
234 location were intermixed with reaches to three probe locations (135°, 180°, and -135).
235 Rotated visual feedback was only provided on trials in which the target appeared at the
236 training location; no feedback was given when the movements were at the probe
237 locations. The test block consisted of 90 reaches, 45 to the training location and 15 to
238 each of the three probe locations. The target sequence was pseudorandomly
239 distributed such that, for every four movements, two were to the training location and
240 two were to probe locations. We restricted the probe locations to those that were most
241 distant to the training location since these are most informative for assessing the
242 reference frame of generalization (see below).

243 The experiment concluded with a final no-feedback block composed of 40 trials,
244 five to each of the eight target locations. Visual feedback was absent during this entire
245 block, providing an assessment of generalization at all locations in the absence of
246 (re)learning.

247 The experimental session lasted approximately 40 minutes.
248

249 *Experiment 2*

250 Twenty participants were assigned to one of two experimental groups, the
251 ENDPOINT-TWO and RETURN-TWO groups, with 10 participants per group. The
252 baseline blocks were the same as in experiment 1. In the rotation block, participants
253 were trained with the rotation at two locations (0° and -45°), with 20 trials at each

254 location. In the test block, reaches to these two locations were pseudorandomly
255 interspersed with trials to the three probe locations. Following the rotation block,
256 participants experienced the no-feedback block composed of 40 trials, five to each of
257 the eight target locations, to assess generalization at all target locations.

258 For the ENDPOINT-TWO group, participants received only endpoint feedback of
259 the movement, similar to the ENDPOINT group from experiment 1. For the RETURN-
260 TWO group, participants received online feedback throughout the entire movement,
261 similar to the RETURN group from experiment 1. Feedback was provided at all
262 locations during the baseline blocks and only for movements to the two training
263 locations in the rotation and test blocks.

264

265 *Data analysis*

266 Kinematic and statistical analyses were performed with Matlab (MathWorks,
267 Natick, MA). To assess adaptation and generalization, we focused on the initial
268 heading angle of the hand. Each movement trajectory, regardless of the actual target
269 location, was rotated to a common axis with the target location at 0°. A straight line was
270 connected between referent points 1 cm and 3 cm along the trajectory, and we
271 computed the angle between this line and the 0° reference line. With this convention,
272 positive angles indicate a positive deviation along the y-axis and negative angles
273 indicate a negative deviation along this axis. To compute the rate of adaptation, we fit
274 the time series of heading angles in the rotation block with an exponential function using
275 the simplex method (Nelder and Mead 1965). The adaptation rate and final asymptotic
276 values are reported in the results.

277 We also computed the curvature of each movement in order to assess the
278 presence and form of corrective movements. Movement curvature was defined as the
279 total absolute curvature in Cartesian coordinates:

$$280 C = \frac{|v_x a_y - v_y a_x|}{(v_x^2 + v_y^2)^{3/2}}$$

281 where v_x and v_y are the x- and y-components of velocity, and a_x and a_y are the x- and y-
282 components of acceleration. Velocity and acceleration were computed using a 4th
283 order Savitsky-Golay filter. This filter introduces less noise than basic difference

284 differentiation (Savitzky 1964; Smith, Brandt et al. 2000).

285 Movement onset was defined by identifying the maximum velocity and scanning
286 the kinematic record backward to determine the last sign reversal in the velocity record.
287 For the ONLINE and ENDPOINT groups, movement time was defined as the interval
288 between movement onset and the time at which the hand crossed the target ring. For
289 the CORRECTIVE and RETURN groups, movement time was quantified as the interval
290 between movement onset and the time at which any part of the feedback cursor
291 overlapped the target circle.

292 We report the mean and the 95% confidence interval of the mean for all dependent
293 variables subjected to statistical evaluation.

294

295 *Modeling*

296 We simulated generalization functions using a radial basis function network
297 (Tanaka, Sejnowski et al. 2009). Identical basis units were employed for all four groups,
298 with the units defined by wrapped Gaussian functions that encoded hand-centered
299 reach directions:

300 (1)
$$g_n^i(\theta_n^{desired}) = a + \frac{1}{\sqrt{2\pi\sigma^2}} \sum_{k=2\pi}^{2\pi} \exp\left(-\frac{(\theta_n^{desired} - \theta^i)^2 + k}{2\sigma^2}\right)$$

301

302 The activity for unit (*i*) on trial (*n*) is dependent on the difference between that unit's
303 preferred direction (θ^i) and the desired target direction ($\theta_n^{desired}$). Each unit in the
304 network has the same tuning breadth (σ) and baseline activity (a). We employed a
305 wrapped Gaussian function because it equates angles separated by 2π (e.g., $0 = 2\pi$).

306 The population-based vector for the desired reach direction ($\bar{r}_n^{desired}$) is given by the
307 sum of the weighted (*w*) activity of each unit (inner product):

308 (2)
$$\bar{r}_n^{desired} = \sum_{i=0}^{2\pi} \vec{w}^i g^i(\theta_n^{desired}) = WG(\theta_n^{desired})$$

309 We used a gradient-descent learning rule to change the weights (*w*), where each weight
310 was adjusted based upon the degree of its activity and the observed error.

311 Models of error-based learning need to consider when the error is generated. In

312 many studies of visuomotor adaptation, the error is defined at a single point in time -- for
 313 example, when the movement amplitude equals the target distance or at the terminal
 314 location of the movement when participants make a single, outbound reach (Tseng,
 315 Diedrichsen et al. 2007; Izawa and Shadmehr 2011). At the other extreme, feedback
 316 information, at least when on-line feedback is available, could provide a continuous
 317 error signal. We opted to employ an intermediate approach, considering two, discrete
 318 error signals, one used to update the weights based on errors observed during the
 319 outbound phase of the movement, and a second used to update the weights on the
 320 corrective, or return phase of the movement (see below). For the ENDPOINT and
 321 ONLINE groups, only the outbound error was used to update the weights (eqn. 3). For
 322 the CORRECTIVE and RETURN groups, both the outbound (eqn. 3) and
 323 corrective/return errors (eqn. 4) were used to update the weights. The two error signals
 324 were modulated by their own learning rate η :

$$325 \quad (3) \quad \Delta W_{outbound} = -\eta_1 G(\theta_n^{desired}) e_{outbound}$$

$$326 \quad (4) \quad \Delta W_{correction/return} = -\eta_2 G(\theta_n^{correction/return}) e_{correction/return}$$

328 The error (eqn. 6) for the outbound portion of the movement was defined as the
 329 difference between the desired movement direction (eqn. 2) and the target direction
 330 (eqn. 5) at the onset of the movement:

$$331 \quad (5) \quad \vec{r}_n^{\text{target}} = \begin{bmatrix} \cos(\theta_n^{\text{target}}) \\ \sin(\theta_n^{\text{target}}) \end{bmatrix}$$

$$332 \quad (6) \quad e_{outbound} = R\vec{r}_n^{desired} - \vec{r}_n^{\text{target}}$$

333
 334 To simulate the rotation, the desired reach vector was rotated by a rotation matrix,
 335 where $\phi = 30^\circ$:

$$336 \quad (7) \quad R = \begin{bmatrix} \cos(\phi) & \sin(\phi) \\ -\sin(\phi) & \cos(\phi) \end{bmatrix}$$

337 The error for the corrective portion of the movement was defined similar to the outbound

338 error (eqn. 9), but here the desired movement direction (eqn. 2) was based on required
339 direction for the correction to the target location or the return movement to the home
340 position (eqn 8):

$$(8) \quad \vec{r}_n^{correction/return} = \begin{bmatrix} \cos(\theta_n^{correction/return}) \\ \sin(\theta_n^{correction/return}) \end{bmatrix}$$

$$(9) \quad e_{correction/return} = R\vec{r}_n^{desired} - \vec{r}_n^{correction/return}$$

343

344 For the RETURN group, the $\theta_n^{correction/return}$ direction was set to 180°. For the
345 CORRECTIVE group, different directions were simulated to determine the direction of
346 the correction that resulted in the appropriate pattern of generalization (see results).

347 Note that only a single time point was used for each error term. In reality, there is
348 a continuous error signal. While it is unknown if control processes use a continuous
349 process, our choice here was motivated by two considerations. First, using discrete
350 samples greatly simplifies the modeling work, especially since a continuous error signal
351 requires making an assumption about the desired trajectory. Second, our main interest
352 here is to test of a proof of concept regarding the potential impact of different feedback
353 signals on generalization. As such, the inclusion of two discrete samples, one for the
354 initial, outbound phase of the movement and the other for the corrective/return phase,
355 should suffice. It is important to note that our model does not represent a time series of
356 heading directions but rather only two distinct time points for the heading direction, one
357 time point for the heading direction of the outbound phase and one for the
358 corrective/return phase. To simulate the outbound phase, the units generate a
359 population vector specifying a single heading direction for the entire outbound phase of
360 the movement. The difference between this heading angle and the target angle specify
361 the outbound error. This error was applied to all of the units; based upon the gradient
362 learning rule (eqn 3), only the weights associated with the units that were highly
363 activated would be significantly altered. To simulate the corrective/return phase, a
364 population vector is generated to specify the heading direction for the corrective/return
365 phase of the movement. The difference between this heading angle and the angle of
366 correction to the target or start position specified the corrective/return error. This error

367 was then applied to all of the units in a similar manner as for the outbound error. Thus,
368 there are only two time points for updating throughout the movement.

369 To generate trajectories for plotting purposes, the two heading directions can be
370 multiple by a time vector to mimic actual movement time. Note that we did not directly
371 compare observed trajectories with model-produced trajectories because our fitting
372 procedure only compares the observed and predicted heading angles (see below).
373 While the model could be set to use any number of time points and thus generate full
374 trajectories, this becomes computationally intractable, leading us to adopt the two-time
375 point simplification. A similar simplification has been used in previous studies, but only
376 using one time point to update movements (Throughman and Shadmehr 2000;
377 Thoroughman and Taylor 2005; Tanaka, Sejnowski et al. 2009).

378 The best fitting parameters of the model were found by a nonlinear least squares
379 fitting procedure based on the Gauss-Newton method. This procedure was set up to
380 minimize the averaged heading angle for each group for the first movement to each
381 target during the no-feedback block. Heading angle was calculated as the difference
382 between a line from the start position to the target location and a line with endpoints
383 based on hand position, 1 and 3 cm into the movement. We constrained parameters a ,
384 σ , $\eta_{outbound}$ to take on a single value for all four groups. Parameters $\theta_n^{correction/return}$ and
385 $\eta_n^{correction/return}$ were allowed to differ for the CORRECTIVE and RETURN groups. For
386 experiment 2, the parameter values for the ENDPOINT and RETURN groups were held
387 constant for the model simulations. The model was trained nearly identical to
388 experiment 1, except that there were two training locations during the rotation block and
389 the test block.

390

391 **Results**

392

393 **Experiment 1**

394 *Kinematic differences between feedback groups prior to rotation training*

395 We first sought to determine how feedback might alter movement kinematics in the
396 absence of a rotation. As described above, participants in the CORRECTIVE and
397 RETURN groups were required to hit the target. In contrast, for participants in the

398 ENDPOINT and ONLINE groups, the trial ended when the hand passed the target ring.
399 Since the second baseline block included reaches to all eight targets, with and without
400 feedback, we focused on these data to asses the effect of feedback on movement time
401 and curvature.

402 Average movement times were within the 300-500 ms time window for both
403 feedback present and feedback absent trials in all four groups (Table 1). A 2-way
404 ANOVA revealed no effect of Feedback (present/absent) ($F_{1,36}=2.17$, $p = 0.15$).
405 However, there was a significant effect of Group ($F_{3,36}=6.85$, $p = 0.004$). Movement
406 times were progressively longer as the amount of feedback increased, becoming
407 especially pronounced in the groups that were required to hit the target. A similar
408 pattern was observed in the evaluation of movement curvature: The degree of
409 movement curvature was similar for Feedback Present and Feedback Absent trials
410 ($F_{1,36}=0.06$, $p = 0.98$), while the effect of Group was reliable ($F_{3,36}=2.68$, $p = 0.05$).
411 Participants in the CORRECTIVE and RETURN groups had more movement curvature,
412 presumably due to the fact that these participants had to make corrective, secondary
413 movements when the initial trajectory failed to terminate at the target. Consistent with
414 this assumption, the curvature differences appear to be limited to the latter phase of the
415 movements since the Group effect was not significant in an analysis of heading angles,
416 ($F_{1,36}=2.17$, $p = 0.10$).

417 An additional comparison of baseline performance was restricted to the data from
418 the RETURN group. For this group, the feedback cursor was visible during both the out
419 and back phases of the movement on the feedback trials. On the no-feedback trials ,
420 the return movement was guided by the contracting ring. Despite this pronounced
421 methodological difference, the duration of the return movement was similar for the two
422 groups ($t_0=1.59$, $p = 0.15$). Indeed, when all four groups were considered, there was no
423 difference in the duration of the return movement between groups ($F_{3,36}=1.08$, $p = 0.37$).
424
425

426 *Kinematic differences during and following rotation training*

427 Following baseline training, the rotation block was introduced. A 30°
428 counterclockwise (CCW) was imposed for 40 movements, all of which were made to a

429 single target at 0°. Rapid adaptation was observed in all four groups, with the final
430 heading angles falling short of the full rotation (Figure 2). An exponential function was
431 fit to the time series of heading angles for each participant in each group. There was no
432 difference in final degree of adaptation ($F_{1,36}=1.33$, $p = 0.28$) nor adaptation rate
433 ($F_{1,36}=0.79$, $p = 0.51$), suggesting that differences in feedback conditions did not
434 significantly affect the course of adaptation (Table 1).

435 After this short adaptation phase, participants were tested on the test block in
436 which three distant probe locations (135°, 180°, -135°) were intermixed with the training
437 location (0°). Feedback was limited to the training location. Changes from baseline in
438 the heading angles to the probe locations provide a signature of generalization (Figure
439 3). These data reveal subtle, but important differences between the groups in the
440 pattern of generalization at the probe locations. Main effects were reliable for the
441 factors Group ($F_{3,36}=6.55$, $p < 0.001$) and Probe Location ($F_{2,72}=6.22$, $p = 0.003$). The
442 average trajectories to the probe targets in the ENDPOINT and ONLINE groups were
443 biased downward in the workspace, a change that is opposite to the rotational direction
444 observed at the trained location. In contrast, participants in the RETURN group showed
445 generalization consistent with the direction of the rotation at the trained location. Across
446 all four groups, generalization was larger at the 135° location compared to the other two
447 locations. The Group x Probe Location interaction was not significant ($F_{1,9}=0.49$, $p =$
448 0.81). To determine if these results may be driven, at least in part, by differential group
449 biases in the second baseline block (where feedback and no feedback trials were
450 interleaved), we subtracted the average heading angle in the baseline block from the
451 average heading angle in the test block for each target location. Similar to the
452 uncorrected analysis, the effects of Group ($F_{3,36}=6.67$, $p = 0.004$) and Probe location
453 were reliable after this correction ($F_{2,72}=4.77$, $p = 0.01$), and the interaction was not
454 significant ($F_{1,9}=0.47$, $p = 0.83$).

455 Figure 4 displays the group means of the heading angles for the training location
456 and probe locations. For the latter, we averaged across the three probe locations given
457 that the interaction term was not reliable and the direction of the generalization was
458 internally consistent within each group. While all four groups showed similar changes in
459 heading angle at the trained location, reflecting consistent adaptation, these summary

460 data make clear the qualitative differences in generalization between the groups. The
461 mean heading angles are in the opposite direction of the rotation for the two groups that
462 were not required to hit the target (ENDPOINT and ONLINE). In contrast, the heading
463 angle was in the direction of the rotation for the group that had feedback during the
464 outbound and return phases of the movement (RETURN). As can be seen in the
465 individual data (dots), there was little overlap in the generalization values between the
466 groups.

467 During the no-feedback block, feedback was never presented and movements
468 were made to all eight locations, allowing a probe on full generalization in the absence
469 of error-driven learning. Figure 5 shows the average trajectories across participants,
470 based on the first movement to each target during the no-feedback block. These
471 trajectories were used to generate the generalization functions depicted in Figure 8, with
472 which the model was trained to fit. All four groups show similar generalization for
473 targets near the training location (for locations 45° and -45°: Group $F_{3,36}=1.01$ p < 0.39;
474 Location $F_{1,36}=0.01$, p<0.97; Interaction $F_{1,9}=0.26$ p < 0.85). No generalization was
475 observed at the vertical locations (90° and -90°: Group $F_{3,36}=0.06$ p < 0.98; Location
476 $F_{1,36}=2.04$, p<0.16; Interaction $F_{1,9}=0.79$ p < 0.50). For targets far from the training
477 location, the no-feedback block results were similar to that observed in the test block,
478 although the location effect was no longer significant (locations 135°, 180°, and -135°:
479 Group $F_{3,36}=7.93$ p < 0.0001; Location $F_{2,72}=2.03$, p<0.14; Interaction $F_{1,9}=0.38$ p <
480 0.88). We expected that generalization would be somewhat attenuated during the no-
481 feedback block given that there should be decay of adaptation with repeated
482 movements without visual feedback.

483

484 *Modeling*

485 The radial basis-function model (eqns. 1-9) was used to simulate reaches during
486 the baseline, rotation, test, and initial cycle of the no-feedback blocks. The parameters
487 of the model were fit using nonlinear least squares approach, minimizing the average
488 target error for each of the four groups during the first cycle of the no-feedback block.
489 The model was initialized with randomized weights and trained for 96 movements,
490 reaching to each target 12 times in the absence of a rotation. A separate weight matrix

491 was used for each group, thus the weight matrices could differ at the start of the rotation
492 training block. The error signal(s) were used to adjust the weight matrix and by the end
493 of the simulated movements in the baseline block the model was successful in reaching
494 to each target with essentially no error (Figure 7 - black). Note that while having
495 different randomized weights, the models for the ENDPOINT and ONLINE groups
496 conditions converged because they are trained with the same outbound error and are
497 not influenced by the corrective/return error term.

498 Following the baseline block, the rotation was imposed for 40 trials, with all
499 reaches limited to the training direction of (0°). The model rapidly learned to adjust the
500 heading angle to compensate for the rotation (Figure 6 - dashed). To simulate the test
501 block, the rotation remained in place on trials in which the target appeared at the
502 training location and the observed errors were used to update the weight matrix.
503 Updates were not made following reaches to the probe locations since feedback was
504 withheld on these trials. Following the test block, the weight matrix was fixed and
505 movements to each target were simulated to assess generalization at all target
506 locations (one cycle of the no-feedback block). Thus, the model simulated the time
507 series of reaches throughout every block, including the rotation and test block, as well
508 during the first epicycle of the washout block.

509 By the end of this simulated training, the model's trajectories for the ENDPOINT
510 and ONLINE conditions are identical since they use the same error, and closely match
511 the hand trajectories for each group (Figure 7 – blue, cyan). The generalization function
512 for these groups provides an excellent match to the data (Figure 8 – blue, cyan, Table
513 2). Significant generalization is observed at $+45^\circ/-45^\circ$, the targets near the training
514 direction, and the pattern here is very similar across the four groups. Little
515 generalization is observed at $+90^\circ/-90^\circ$. Generalization at these locations is primarily
516 driven by the width of the basis function. The estimated value of this parameter (σ) was
517 16° , a value that is slightly narrower than previously estimated (Tanaka, Sejnowski et al.
518 2009).

519 Generalization is not only driven by the width of the neural tuning function, but is
520 also dependent on baseline activity of the simulated units (Thoroughman and Taylor
521 2005; Ingram, Howard et al. 2011). The estimated baseline activity was quite small

522 (a=0.04). Nonetheless, this small level of activity was sufficient to produce some degree
523 of generalization at all locations. Importantly, the positive baseline activity produces
524 generalization in a direction consistent with a Cartesian representation of the error, not
525 in a rotational frame of reference. Thus, the positive baseline activity produces the
526 downward generalization at the probe locations for the ENDPOINT and ONLINE
527 conditions (Figure 7 - blue, cyan).

528 The positive baseline activity will also produce downward generalization effects for
529 the CORRECTIVE and RETURN conditions. However, the generalization pattern for
530 these groups is also influenced by the second error term used to guide the movements
531 to the target and/or start location. That is, the weights for the RETURN and
532 CORRECTIVE models are adjusted twice on each trial, once based on the outbound
533 error and a second time based on the return movement error. The inclusion of this
534 second error term led to very different patterns of generalization compared to that
535 observed for the ENDPOINT and ONLINE groups (Figure 7 – purple, red). In particular,
536 for the 180° direction, the trajectory was now shifted in the same rotational direction as
537 at the training location. Note that the effect of this second error term counteracts the
538 direction of generalization induced by the positive baseline activity.

539 For the CORRECTIVE and RETURN conditions, we had to specify the direction of
540 the corrective movement ($\theta_n^{corrective}$). The best fit for both groups arises when the
541 planned direction at the time of the second error update is 180°. When other directions
542 were considered, such as -90° and -135°, the fits of the generalization curves for other
543 directions of the corrective movement was much poorer (e.g., -180: RMS = 1.99; -90°:
544 RMS = 2.12; -135°: RMS = 2.91). The 180° direction seems reasonable for the
545 RETURN group since these participants must move in this general direction to return to
546 the start location. It is more surprising that 180° value also provides the best fit for the
547 CORRECTIVE group since movements in this direction would only occur when the
548 participants overshot the target. Participants in the CORRECTIVE group did overshoot
549 early in rotation training, with the mean amplitude 0.8 ± 0.02 cm beyond the target during
550 the first eight reaches to the training location. This tendency decreased over the course
551 of training, with the mean overshoot only 0.07 ± 0.006 cm over the last eight movements
552 of rotation training ($t_9=5.50$, $p<0.001$).

553 We allowed the model to estimate separate learning rates for the second error
554 signal for the RETURN and CORRECTIVE groups given that these error signals were
555 used for different purposes. Three points are of note here. First, the learning rates for
556 the second error signal are considerably smaller than the learning rate for the outbound
557 error signal, presumably reflecting the fact that the compensation for the rotation is
558 based on an error associated with the initial heading direction. Second, the estimated
559 learning rate for the RETURN group is larger than that estimated for the CORRECTIVE
560 group, perhaps due to the large error that occurs when the heading for the return
561 movement is again perturbed by the rotation. Third, the inclusion of separate learning
562 rates for the second error signal provided a much better fit of the generalization
563 function. Overall, the full 5-parameter model provides an excellent fit of the
564 generalization function for these groups (Figure 8, Table 2), accounting for 61% of the
565 unexplained variance from the fit obtained with a simpler 3-parameter model (from
566 $r^2=0.89$ to 0.96 in the CORRECTIVE condition and 0.89 to 0.93 in the RETURN
567 condition).

568

569 **Experiment 2**

570 A central feature of the model is that the current error information is used to
571 modify the synaptic weights of the network elements in a manner proportional to the
572 level of activity of the directionally-tuned units that are active at the time of the update.
573 When the movement is made with endpoint-only feedback, only units tuned to the
574 direction of the target are significantly activated, and thus error-based training is specific
575 to those units. However, when corrective movements are made, or when feedback is
576 provided when the participant returns to the start location, units tuned in other directions
577 can be active, resulting in training in those directions leading to what would be
578 measured as a change in generalization. Thus, the pattern of generalization will
579 depend on the range of units that are activated when feedback is available.

580 This architecture predicts that the generalization function should be modified if
581 the set of training locations is increased. Moreover, the form of this function should be
582 modified in a specific manner. Consider a condition in which the training set includes
583 two locations, 0° and -45° , and feedback is provided on the outbound and return

584 movement. Adaptation should not only be observed for movements around these two
585 training locations, but should also be evident during generalization for movements to
586 targets at 180° and 135°, the movement directions that are required to return to the start
587 location.

588 We simulated this two-training target condition using the model parameters for
589 the RETURN condition from experiment 1. During the training block, the model used
590 outbound errors generated for reaches to the 0° and -45° target locations and return
591 errors for reaches towards the start location, movements that involved trajectories that
592 corresponded to that required for reaches in the direction of the 180° and 135° targets.
593 The model readily adapted to both training locations. Importantly, the model showed
594 similar generalization around the 180° target and 135° target (Figure 9A - orange).
595 Thus, the spread of generalization is not only larger when there are two targets
596 compared to training at only a single target (Figure 9A - red dashed), but the form of
597 generalization was in a specific manner for targets distant to the training locations. To
598 confirm that this change in the generalization function was not simply due to training at
599 two locations, we simulated a two target condition in which feedback was only given at
600 the endpoint of the outbound movement, using here the model parameters from the
601 ENDPOINT condition of experiment 1. For this simulation, the model predicted a very
602 different pattern of generalization (Figure 9B - dark purple), similar to that predicted
603 when only one training target is used (Figure 9B - blue dashed).

604 To empirically test this prediction, we recruited two more groups of participants
605 who were presented with targets at two locations during the rotation phase. One group
606 was provided with continuous on-line feedback during both the outbound movement and
607 the return (RETURN-TWO group), whereas the other group only received feedback at
608 the end of the reach (ENDPOINT-TWO group). Both groups adapted to the rotation at
609 both training locations (Figure 10A). However, they exhibited very different patterns of
610 generalization during the test block (Figure 10B,C). The RETURN-TWO group showed
611 generalization in the clockwise direction (rotational reference frame) and the magnitude
612 of this effect at the 135° location is larger than that observed for the RETURN group
613 from experiment 1 (Figure 10B; $t_{18}=3.10$, $p = 0.006$). In contrast, the ENDPOINT-TWO
614 group showed generalization that was similar to that observed in the ENDPOINT group

615 from Experiment 1 (compare Figure 3A and 10C). In particular, the generalization at the
616 probe locations was in the counter-clockwise direction (or downward). No differences
617 were observed between the ENDPOINT-TWO (Exp. 2) and ENDPOINT (Exp. 1)
618 conditions in a between-experiment comparison ($t_{18}=0.62$, $p = 0.55$). In summary, the
619 observed results closely conform to the predictions of the model.

620

621 **Discussion**

622

623 In previous studies of visuomotor rotation, generalization has been found to be in
624 the same angular direction of the rotation, leading to the idea that participants develop
625 an internal model of the perturbation (Pine, Krakauer et al. 1996; Krakauer, Pine et al.
626 2000). In the present study, we find that the shape of the generalization function is
627 strongly influenced by the type of visual feedback provided during adaptation. When
628 participants were required to make on-line corrections to terminate the movement within
629 the target (and during a return movement to the starting location), the pattern of
630 generalization near the training location and at far locations was consistent with the
631 hypothesis that participants had indeed learned a rotational transformation. However,
632 the generalization function was not monotonic, with minimal evidence of learning at
633 directions orthogonal to the training location. Even more striking, when on-line
634 corrections were not required, the angular direction of the generalization function was
635 reversed: heading errors at these locations were in the opposite direction of the rotation,
636 a pattern consistent with generalization in an exocentric reference frame. These
637 different task demands yielded subtle, yet important differences, leading us to
638 reconsider the processes that drive generalization.

639 We were able to capture these discrepant patterns of generalization in a unified
640 model that emphasizes the important contribution of error information for adjusting the
641 output of movement units defined by a radial-basis function network (Thoroughman and
642 Shadmehr 2000; Thoroughman and Taylor 2005; Tanaka, Sejnowski et al. 2009).
643 Generalization was defined by three components: 1) the neural tuning width, 2) neural
644 baseline activity, and 3) the error signals experienced by the system during adaptation
645 (Figure 11). In previous computational studies of generalization, the focus has been on

646 the first two factors that define the shape of the tuning function. Different patterns of
647 generalization observed across several task domains (e.g., rotations, translations, gain
648 changes) have been attributed to differences in the shape of the tuning functions
649 (Ghahramani, Wolpert et al. 1996; Thoroughman and Taylor 2005; Tanaka, Sejnowski
650 et al. 2009; Pearson, Krakauer et al. 2010). We find that careful consideration of the
651 error signal is sufficient to account for qualitative changes in generalization without
652 requiring variation in the shape of the tuning function. Indeed, applying a consistent set
653 of principles across task conditions can yield different patterns of generalization from a
654 uniform set of tuning functions, a desirable feature given that the basic task-- adaptation
655 of a sensorimotor map-- remains constant. Thus, differences in generalization need not
656 be attributed to differences in the neural representation per se, but rather reflect
657 constraints imposed by the available error information.

658 Recent work by the Brayanov and Smith (2011) have suggested that
659 generalization functions reflect the composite operation of two processes (Brayanov,
660 Petreska et al. 2011). One process is local in nature, limited to directions similar to the
661 training direction(s), and is manifested in a Cartesian reference frame. The second
662 process is global affecting all directions and is manifested in a rotational reference
663 frame. This two-process model is at odds with our model in that we postulate a single
664 process, one where the units code movement direction in a rotational space but receive
665 an error that is based in a Cartesian reference frame. However, as emphasized in the
666 current study, it is important to consider the type of feedback presented during the
667 training phase. Brayanov and Smith (2011) provided online feedback throughout the
668 movement, requiring that the cursor to land in the target region. This form of feedback
669 will provide error information at multiple states, depending on the duration of the
670 movement. This is similar to our CORRECTIVE group (or our RETURN group), where
671 we see either no generalization or rotational generalization at targets far from training.
672 Any differences in our CORRECTIVE group and the work by Brayanov and Smith
673 (2011), could be due to differences in the speed of movements, time allowed for online
674 corrections, and how generalization is tested during training. Participants receive error
675 feedback at many states (positions) during the corrective feedback portion of the
676 movement and, according to our model, these additional states during this period also

677 contribute to learning thereby leading to differences in generalization. Thus, any test of
678 generalization may be contaminated by error-based feedback if it is available during
679 training. The pattern of generalization will be different depending on the number of
680 states that are visited and the duration of the reach that involves traveling through
681 states that are not directed towards the target.

682

683 *Tuning functions limit the degree of generalization*

684 Prior studies have generally observed relatively narrow generalization functions.
685 Substantial generalization is observed near the direction of training, and falls off rapidly
686 as the direction of probe movements deviates from the training direction (Krakauer, Pine
687 et al. 2000; Tanaka, Sejnowski et al. 2009). The shape of this generalization function
688 has been attributed to the shape of neuronal tuning functions in a radial basis-function
689 network (Thoroughman and Shadmehr 2000). These functions can be approximated by
690 a Gaussian, tuned to movement velocity (or direction). The output of the network is the
691 weighted sum of these velocity-tuned units, the population vector (Georgopoulos,
692 Schwartz et al. 1986). When a perturbation is introduced, the weights are adjusted
693 based on an error signal defined by the difference between the planned and observed
694 direction of movement. Stable performance is achieved with a gradient descent
695 learning rule in which the weights are adjusted proportionally to the size of the error and
696 the unit's level of activity.

697 In such models, the extent of generalization is constrained by the standard
698 deviation or width of the Gaussian function (Figure 11). Thus, weight adjustments are
699 limited to units that were active during the movement. If the width of the Gaussian
700 function is large, more units will be active for any given movement and, as a
701 consequence, generalization will be broad. If the width of the Gaussian function is
702 small, only a few units are active during each movement and generalization is narrow.

703 Previous studies have suggested that the width of the tuning functions are
704 relatively narrow, with estimates ranging from 20° - 30° (Thoroughman and Shadmehr
705 2000; Tanaka, Sejnowski et al. 2009). These estimates suggest that generalization
706 should be of limited extent. While the generalization function does fall off rather sharply
707 from the training direction (e.g., 50% reduction at angles greater than 20°), most studies

708 have also observed some degree of generalization at directions far from the training
709 location (Pine, Krakauer et al. 1996; Krakauer, Pine et al. 2000; Tanaka, Sejnowski et
710 al. 2009). One proposal to account for distant generalization involves the use of more
711 complicated tuning functions such as a cosine-tuned function or one involving a
712 difference of Gaussians (Thoroughman and Taylor 2005). Functions such as these
713 have been identified in the motor cortex (Georgopoulos, Kalaska et al. 1982),
714 cerebellum (Coltz, Johnson et al. 1999), and visual cortex (Hubel and Wiesel 1959). An
715 alternative hypothesis is that different subpopulations of neurons have different tuning
716 functions and during learning, error signals are used to select the appropriate
717 subpopulations (Thoroughman and Taylor 2005). Both of these hypotheses require
718 sophisticated neural circuitry for tuning selection and, to date, empirical support for such
719 a learning process has not been identified. While there is evidence of experience-
720 dependent changes in the preferred direction of motor cortex cells (Gandolfo, Li et al.
721 2000; Taylor, Tillery et al. 2002; Paz and Vaadia 2004), consistent changes to the
722 shape of the tuning function have not been identified.

723

724 *Baseline activity produces weak, but broad generalization*

725 We opted to take a different approach here. We assumed that the units could be
726 represented as directionally-tuned Gaussian functions with a fixed tuning width (Tanaka,
727 Sejnowski et al. 2009). As noted above, this model easily captures the fact that
728 generalization is largest around the trained direction. In addition, we found that a
729 parameter representing (nonzero) baseline neural activity was sufficient to produce a
730 modicum of generalization at distant locations (Thoroughman and Taylor 2005; Ingram,
731 Howard et al. 2011). Importantly, this baseline activity does not predict generalization in
732 a rotational frame of reference, but rather in a direction consistent with a Cartesian
733 representation of the error. The presence of baseline activity was critical in reproducing
734 the generalization patterns observed for the ENDPOINT and ONLINE groups.

735 It is unclear if baseline activity should be considered a feature of the tuning
736 functions of the neurons or a distinct, separate process. It is possible that the
737 generalization effects at distant locations reflect the operation of a second learning
738 process. That is, generalization function may be the composite of locally adapted basis

739 tuning functions and a second generic, albeit weaker process that is applied to all units
740 (Pearson, Krakauer et al. 2010). This generic process may reflect the effects of learning
741 at a more abstract level such as an adjustment in a motor plan (Figure 11). For
742 example, after seeing that movements to the training location consistently result in an
743 upward error, the participant may be biased to move in the downward direction, a bias
744 that could be broadcast uniformly across all movement directions.

745 The baseline parameter was fixed for all four groups. While the model with this
746 term was sufficient to account for generalization in the ENDPOINT and ONLINE groups,
747 it failed to provide an adequate fit for the CORRECTIVE and RETURN groups. For
748 these groups, generalization was either minimal at all distant locations or in a direction
749 consistent with the rotation. If the baseline activity were the sole source of the distant
750 generalization, it would be necessary to postulate that baseline activity is influenced by
751 the task demands. As an intrinsic feature of the tuning functions, the baseline activity
752 would have to be subject to some form of experience-dependent plasticity to account for
753 the group differences. Alternatively, if the baseline activity represented a separate
754 process that provided a generic error signal, we would have to propose that this signal
755 varied between groups. This seems unlikely given that all of the groups were trained
756 with the same target and showed very similar adaptation at this location.

757

758 *The importance of error signals during training*

759 To account for the group differences in generalization, we explored the influence of
760 error information, a feature of the model that builds naturally on the different task
761 demands imposed on the four groups. As in standard models of adaptation, the units
762 in our model were updated by an error signal, representing the difference between the
763 desired and actual movement. However, the task demands were more stringent for the
764 CORRECTIVE and RETURN groups. For the former, the movement had to terminate in
765 the target location; for the latter, feedback was also available when the participant
766 returned to the start position. The feedback available to guide these corrections not
767 only provides a source of additional error information, but also is utilized at a time when
768 the dynamics of the network has changed: The pattern of activation across the units in
769 the neural network is altered and, as such, has altered the landscape in terms of which

770 units are eligible for updating. We modeled this by introducing a second error updating
771 epoch for these two groups. The inclusion of this additional error term was capable of
772 generating the generalization curves exhibited by the CORRECTIVE and RETURN
773 groups. The parameter estimates suggest that the error information used for the
774 second update is not as salient for the CORRECTIVE condition compared to the
775 RETURN condition. Note that this difference is how the model accounts for the
776 difference in generalization between the two groups; as such, it cannot be said to be an
777 “explanation”. Nonetheless, the model clearly demonstrates how generalization is
778 influenced by the form of the error information.

779 We recognize that our discrete use of feedback information is a simplification.
780 Differences between the observed and simulated data, especially for the return
781 condition, may be due to undersampling of the error signal given that we limited the
782 updating process to two time points. We expect that the fits would improve if we used
783 more time points. While error information is continuously available, it remains to be
784 seen if updates to the motor commands are provided in a continuous or discrete
785 manner (Flash and Henis 1991; Ijspeert, Nakanishi et al. 2002). The point we wish to
786 emphasize here is that the inclusion of error signals that conform to the basic task
787 demands were sufficient to produce qualitatively different generalization functions. For
788 all four groups, the outbound error adjustment was based on an error defined by the
789 initial heading direction (measured between 1 and 3 cm; see methods). For the
790 CORRECTIVE and RETURN groups, the second error adjustment was applied when
791 the movement was heading in the reverse direction (180° , based on the model fits). We
792 were surprised to find that the best fit for the CORRECTIVE group was obtained when
793 the second error adjustment was applied to units generating trajectories in the 180°
794 direction. A priori, we expected that, given the rotation, the 90° or 135° directions would
795 be more relevant for this group. If the second error term had updated units producing
796 trajectories in these directions, then significant generalization should have been
797 observed for reaches to targets at these directions, a result that was not present in the
798 participants’ generalization curves. It is possible that the return movement, with its
799 prominent 180° direction is especially salient given the need to return to the center
800 location before the next trial. This may produce a greater emphasis on this direction for

801 error updating. Alternatively, error information may be delayed with respect to the units
802 that were responsible for the errors. If this information was not properly maintained in
803 memory, then the system could misapply the error information. Thus, recent errors in a
804 particular direction may be used to update units specifying the current direction,
805 resulting in the wrong errors being applied to the wrong units.

806 Nevertheless, the current data fits and simulations show that using just two error
807 updates, one for the outbound phase and a second for the return phase, can lead to
808 qualitative changes in the generalization function. This point is underscored by the
809 results of experiment 2 where we observed a change in the generalization at specific
810 locations, distant to the training locations. Thus, a simplified model in which the
811 utilization of error information is likely sparser than in reality was sufficient to predict the
812 general shape of generalization functions; we assume a more realistic model would
813 provide even better quantitative fits to bolster these qualitative observations. An
814 important implication of our work is that it may be a misnomer to refer to the trajectory
815 changes for movements to probe locations as “generalization”, at least for the RETURN
816 groups. Generalization implies that a behavioral change is the result of learning a
817 particular task or movement. As the modeling work presented here makes clear, the
818 behavioral changes at probe locations for the RETURN group is the result of a directed
819 movement towards the starting location. Prior studies of generalization have tended to
820 use tasks in which visual feedback was continuously available. As shown here,
821 generalization in these studies is “contaminated” by the utilization of error information
822 during both the outbound and return phases of the movements. Most importantly, the
823 modeling work makes clear that we need not assume different representations to
824 account for task-dependent differences in generalization. Rather, a parsimonious
825 account of these differences is possible when consideration is given to the error
826 information available during learning.

827

828 **Acknowledgements**

829 We are grateful to Maurice Smith and Jordan Brayanov for their many comments
830 throughout the course of this project. We thank Christina Gee for help with data
831 collection and Jon Berliner for help with manuscript preparation. Jordan Taylor was

832 supported by an NRSA fellowship (F32NS064749) from the National Institute of
833 Neurological Disorders and Stroke, and Richard Ivry was supported by 5R01HD060306
834 from the National Institute of Child Health and Human Development.

835

836

837 Figure 1. Different forms of visual feedback for a center-out reaching task workspace.
838 There were 8 target locations. Participants practiced reaching to all locations in the
839 baseline blocks. During the training block, participants only moved to the target at 0°
840 (green target) and a 30° rotation was applied to the cursor. During the test block,
841 participants reached to the training location (with feedback) and the three probe
842 locations (black filled, no feedback). Generalization to all locations was tested in a no
843 feedback block at the end of training. A ring connecting the target locations was visible
844 during the reaches. The trial ended for the ENDPOINT and ONLINE groups when the
845 movement intersected this ring, with feedback limited to the endpoint for the former
846 (Blue) and visible until the hand intersected the target ring for the latter (Cyan). The
847 corrective feedback group (Purple) had online feedback and was required to hit the
848 target to end the movement. The return group (Red) had online feedback during
849 reaches to the target and during the return movement to the starting position.

850

851 Figure 2. Heading angle relative to target direction during baseline (trials 1-96), rotation
852 (97-136), test (137-226), and no-feedback (227-266) blocks. Colors correspond to the
853 four groups: ENDPOINT (blue), ONLINE (cyan), CORRECTIVE (purple), RETURN
854 (red). Movements to the training target location are filled circles and movements to the
855 other locations are open circles.

856

857 Figure 3. Hand trajectories during the baseline block (black) and test block for the four
858 groups: ENDPOINT (blue), B) ONLINE (cyan), C) CORRECTIVE (purple),D) RETURN
859 (red). During this baseline block, feedback was provided at all locations. During the
860 test block, feedback was provided on trials in which the target appeared at the training
861 location. No feedback was provided on trials in which the target appeared at probe
862 locations.

863
864 Figure 4. Group averaged (bars) heading angles relative to target direction for
865 movements to the training and probe locations in the rotation block. Dots indicate
866 individual participant values. Colors correspond to the four groups: ENDPOINT (blue),
867 ONLINE (cyan), CORRECTIVE (purple), RETURN (red).
868
869 Figure 5. Hand trajectories during the baseline block (black) and the first cycle of the no
870 feedback block for the four groups: ENDPOINT (blue), ONLINE (cyan), CORRECTIVE
871 (purple), RETURN (red). Movements were made to all eight locations without feedback.
872
873 Figure 6. Model simulation of training in each feedback condition. The weights were
874 initially randomized and the model learned to reach to each target with feedback in the
875 baseline block. During the rotation block, the model learned to compensate for the
876 rotation (three colored dashed lines are superimposed). Probe targets (colored solid
877 lines) were introduced during the test block (movements 137-226). No-feedback block
878 (open circles) was limited to eight movements (one per target) since the model was now
879 stable given the absence of feedback. ENDPOINT (blue), ONLINE (cyan),
880 CORRECTIVE (purple), RETURN (red). Note that the ENDPOINT and ONLINE groups
881 overlap completely after training block.
882
883 Figure 7. Model simulation of hand trajectories during the baseline block (black) and no
884 feedback block for the four groups: ENDPOINT (blue), ONLINE (cyan), CORRECTIVE
885 (purple), RETURN (red)
886
887 Figure 8. Model fit of generalization function. Average heading angle of the hand at
888 each target location (black circles and solid lines) for each group and the model's
889 heading angle (dashed line). A) EF (blue), B) OF (cyan), C) CF (purple), and D) RF
890 (red) groups.
891
892 Figure 9. Predicted hand trajectories from the model during the baseline block (black)
893 and no feedback block for conditions in which two targets are used during the training

894 block with either online feedback during the outbound and return phases (A: RETURN-
895 TWO, orange) or endpoint only feedback (A: ENDPOINT-TWO, purple). The
896 predictions were derived by using parameters estimated from the data fits for
897 experiment 1 when only one target had been used during training.

898

899 Figure 10. A) Heading angle relative to target direction during baseline (trials 1-96),
900 rotation (97-136), test (137-227), and no-feedback (228-266) blocks. The ENDPOINT-
901 TWO group is in blue and the RETURN-TWO group in orange. Movements to the
902 training target location are filled and movements to the other locations are open circles.
903 B) RETURN-TWO group and C) ENDPOINT-TWO group hand trajectories during the
904 baseline block (black) and test block. As in experiment 1, feedback was only provided
905 when the target appeared at the two training locations (green) in the test block.

906

907 Figure 11. Schematic activity level of directionally tuned units during the outbound
908 (blue) and return (red) phases of a movement to the training target (0°). The
909 generalization function is determined by three components: baseline activity (a), tuning
910 width (σ), and modification of the weights determining the contribution of each unit to
911 the population vector. These weights are updated based on an error signal generated
912 during the outbound phase of the movement for all groups and the return phase for the
913 CORRECTIVE and RETURN groups.

914

915 Table 1. Temporal, kinematic, and learning measures for the four groups. Movement
916 time (s), intertrial interval (s), movement curvature (cm^2), and heading angle (deg) are
917 shown for each group during the baseline phase, with and without endpoint feedback.
918 Learning rate and final asymptotic value are based on exponential fit of the adaptation
919 curve in the rotation training block. The means and 95% confidence interval of the
920 mean are reported.

921

922 Table 2: Parameter estimates and model fits for each group based on the basis function
923 model (Eqns 1-9). a : baseline neural activity; σ : width of the basis function; η_{outbound} :
924 learning rate for the outbound portion of the movement, constrained to be identical for

925 all four groups. $\eta_{\text{corrective}}$ and $\theta_{\text{corrective}}$: learning rate and desired angle of movement for
926 the corrective portion of the movement for the CORRECTIVE group; η_{return} and θ_{return} :
927 learning rate and desired angle of movement for the return portion of the movement for
928 the RETURN group. Fits were quantified by two measures, root mean square error
929 (RMS) and the correlation coefficient between the model simulation and group-
930 averaged heading angle during the no-feedback block.

931

932

933

934

935

936

937

938

939

940

941

942

943

944

945

946

947

948

949

950

951

952

953

954

955

956

957 Table 1

Groups	Movement Time (s)	
	Baseline FB	Baseline No FB
ENDPOINT	0.37±0.02	0.38±0.03
ONLINE	0.39±0.04	0.39±0.04
CORRECTIVE	0.42±0.05	0.39±0.05
RETURN	0.50±0.07	0.43±0.02
Intertrial Interval (s)		
	Baseline FB	Baseline No FB
ENDPOINT	2.13±0.44	1.94±0.35
ONLINE	1.93±0.23	2.04±0.24
CORRECTIVE	2.04±0.39	1.81±0.23
RETURN	2.44±0.40	2.10±0.25
Total Curvature (cm ²)		
	Baseline FB	Baseline No FB
ENDPOINT	15.5±6.97	12.2±8.20
ONLINE	3.12±1.60	5.69±5.47
CORRECTIVE	40.9±21.9	48.9±82.2
RETURN	39.8±32.5	22.7±20.4
Heading Angle (deg)		
	Baseline FB	Baseline No FB
ENDPOINT	0.21±0.82	-0.06±1.22
ONLINE	1.23±1.75	0.84±1.78
CORRECTIVE	0.67±1.24	0.99±1.07
RETURN	1.96±1.13	1.45±0.99
Rotation Training		
	Final Value	Rate
ENDPOINT	-25.8±3.04	3.98±3.24
ONLINE	-25.3±1.68	2.84±1.37
CORRECTIVE	-23.0±1.65	2.35±0.97
RETURN	-24.2±1.64	2.07±0.76

958

959

960

961

962

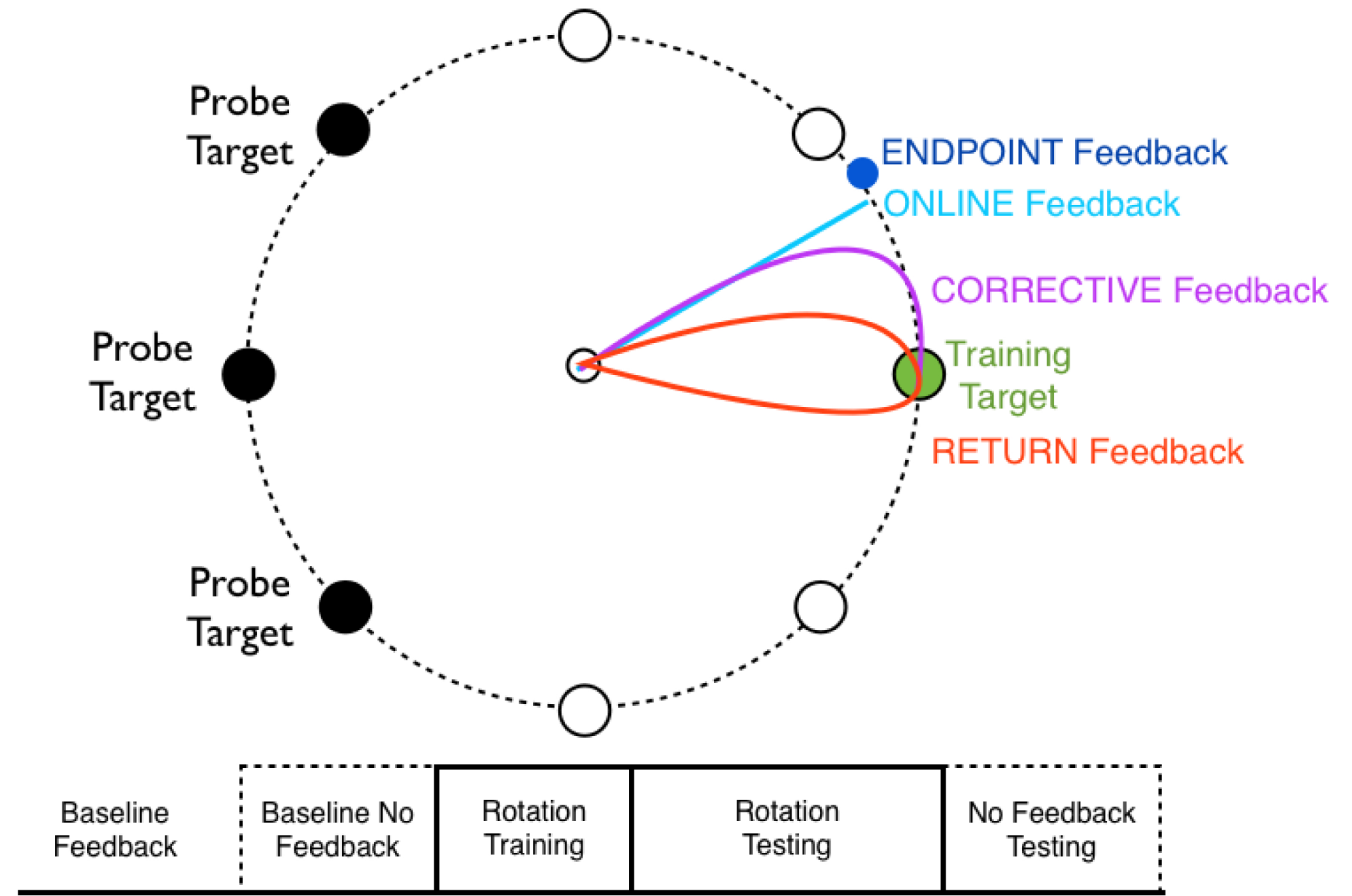
963

Table 2

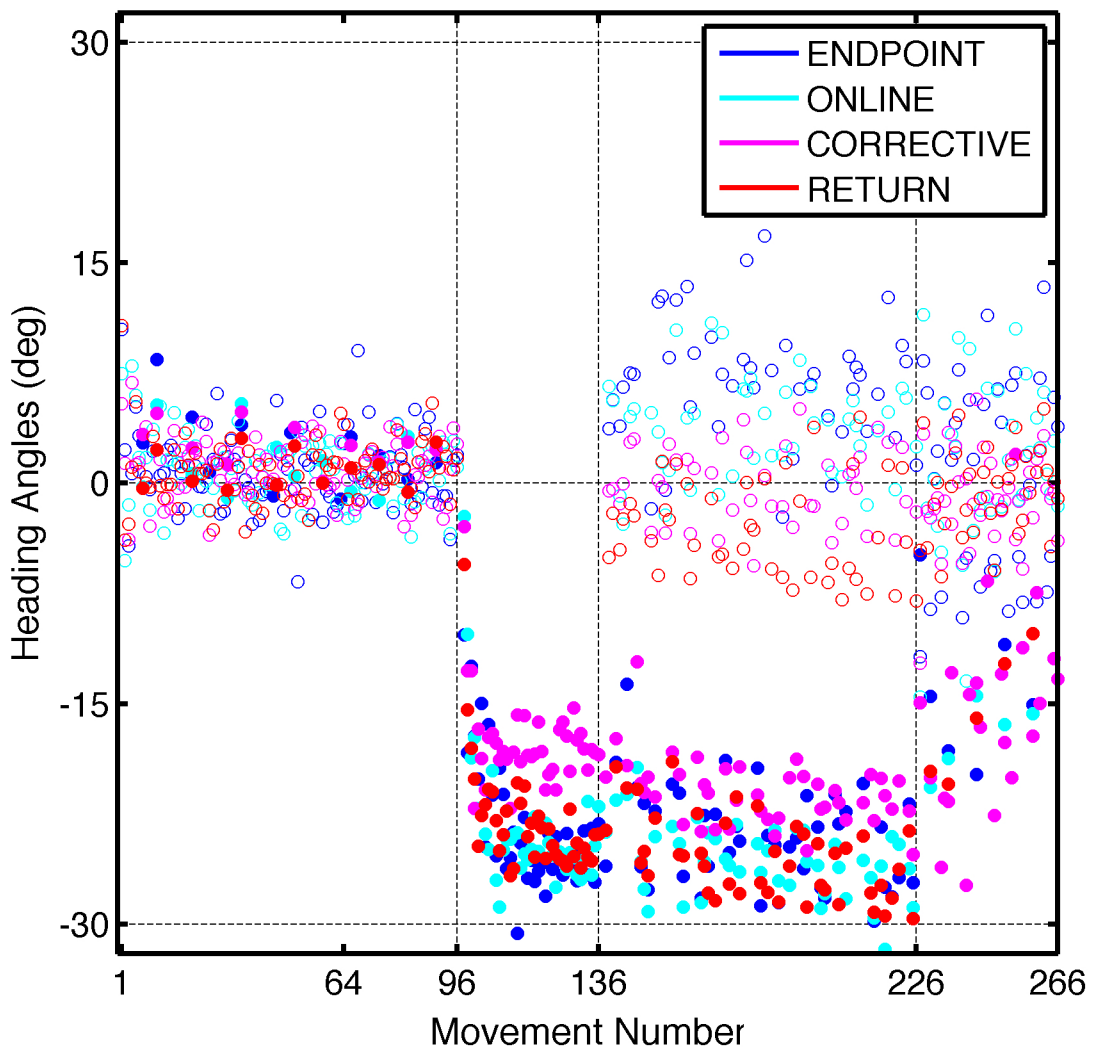
Model Parameters		Model Fit		
			RMS	r^2
a	0.04	ENDPOINT	1.68	0.98
σ	16°	ONLINE	1.50	0.98
η_{outbound}	0.18	CORRECTIVE	1.99	0.96
$\eta_{\text{corrective}}$	0.0007	RETURN	2.40	0.93
η_{return}	0.0017			
$\theta_{\text{corrective}}$	180°			
θ_{return}	180°			

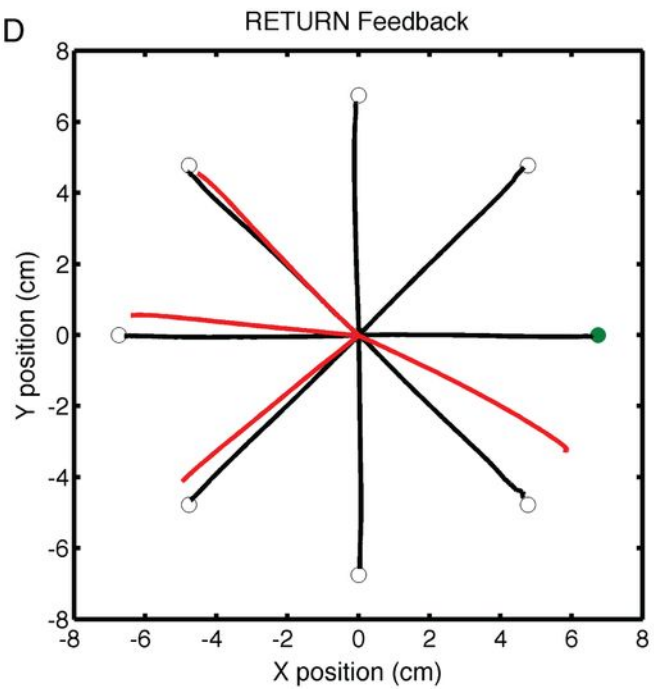
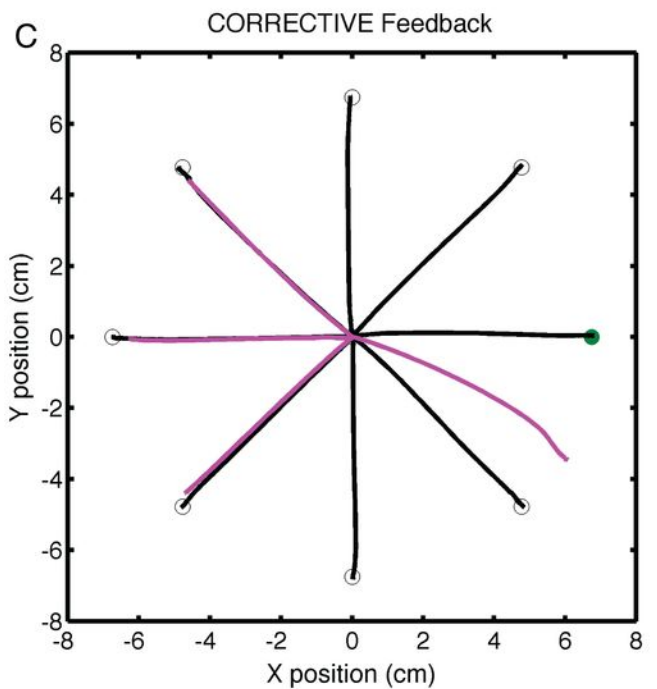
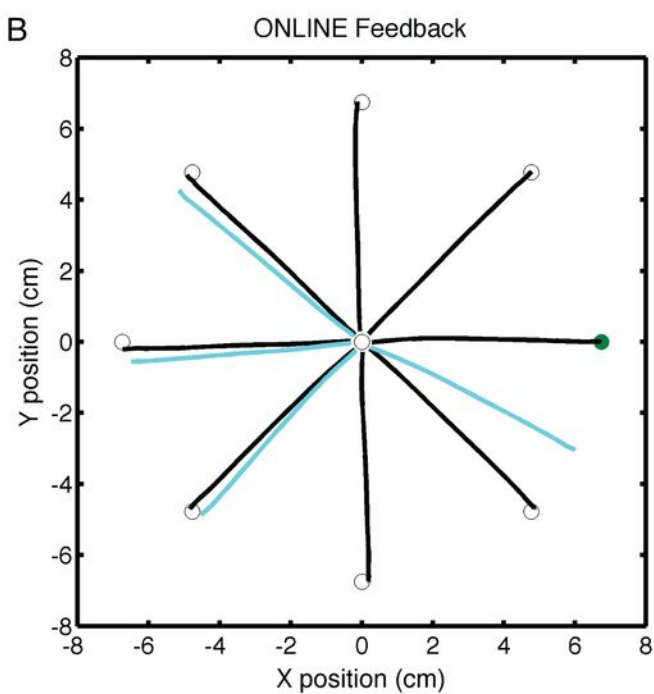
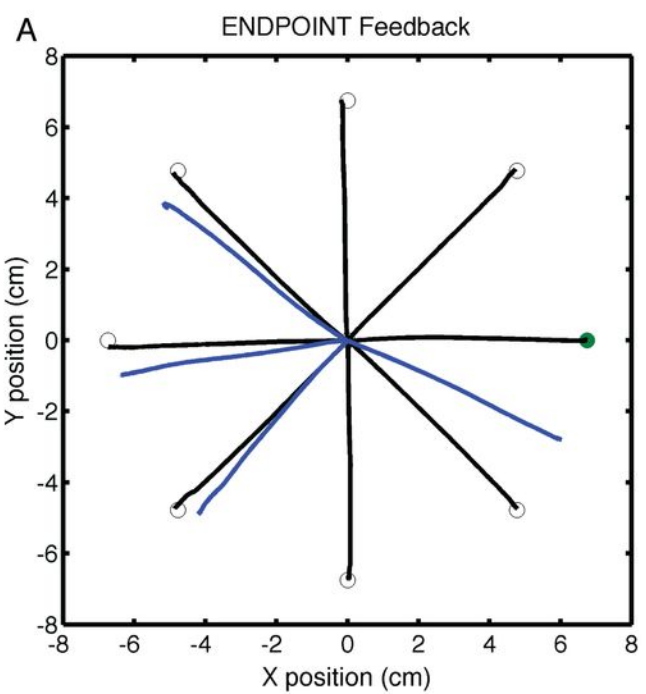
- 966 **Bibliography**
- 967 Brayanov, J. B., B. Petreska, et al. (2011). Visuomotor transformations elicit
968 simultaneous learning in two distinct coordinate systems. Society for
969 Neuroscience Abstract, Washington, D. C. .
- 970 Coltz, J. D., M. T. Johnson, et al. (1999). "Cerebellar Purkinje cell simple spike
971 discharge encodes movement velocity in primates during visuomotor arm
972 tracking." J Neurosci **19**(5): 1782-1803.
- 973 Donchin, O., J. T. Francis, et al. (2003). "Quantifying generalization from trial-by-trial
974 behavior of adaptive systems that learn with basis functions: theory and
975 experiments in human motor control." J Neurosci **23**(27): 9032-9045.
- 976 Flash, T. and E. Henis (1991). "Arm trajectory modification during reaching towards
977 visual targets." Journal of Cognitive Neuroscience **3**: 220-230.
- 978 Gandolfo, F., C. Li, et al. (2000). "Cortical correlates of learning in monkeys adapting to
979 a new dynamical environment." Proc Natl Acad Sci U S A **97**(5): 2259-2263.
- 980 Georgopoulos, A. P., J. F. Kalaska, et al. (1982). "On the relations between the direction
981 of two-dimensional arm movements and cell discharge in primate motor cortex."
982 J Neurosci **2**(11): 1527-1537.
- 983 Georgopoulos, A. P., A. B. Schwartz, et al. (1986). "Neuronal population coding of
984 movement direction." Science **233**(4771): 1416-1419.
- 985 Ghahramani, Z., D. M. Wolpert, et al. (1996). "Generalization to local remappings of the
986 visuomotor coordinate transformation." J Neurosci **16**(21): 7085-7096.
- 987 Hinder, M. R., J. R. Tresilian, et al. (2008). "The contribution of visual feedback to
988 visuomotor adaptation: how much and when?" Brain Res **1197**: 123-134.
- 989 Hubel, D. H. and T. N. Wiesel (1959). "Receptive fields of single neurones in the cat's
990 striate cortex." J Physiol **148**: 574-591.
- 991 Ijspeert, A. J., J. Nakanishi, et al. (2002). "Movement Imitation with Nonlinear Dynamical
992 Systems in Humanoid Robots." IEEE International Conference on Robotics and
993 Automation(2002): 1398-1403.
- 994 Ingram, J. N., I. S. Howard, et al. (2011). "A single-rate context-dependent learning
995 process underlies rapid adaptation to familiar object dynamics." PLoS Comput
996 Biol **7**(9): e1002196.
- 997 Izawa, J. and R. Shadmehr (2011). "Learning from sensory and reward prediction errors
998 during motor adaptation." PLoS Comput Biol **7**(3): e1002012.
- 999 Krakauer, J. W., Z. M. Pine, et al. (2000). "Learning of visuomotor transformations for
1000 vectorial planning of reaching trajectories." J Neurosci **20**(23): 8916-8924.
- 1001 Nelder, J. A. and R. Mead (1965). "A Simplex Method for Function Minimization." The
1002 Computer Journal **7**(4): 308-313.
- 1003 Oldfield, R. C. (1971). "The assessment and analysis of handedness: the Edinburgh
1004 inventory." Neuropsychologia **9**(1): 97-113.
- 1005 Paz, R. and E. Vaadia (2004). "Learning-induced improvement in encoding and
1006 decoding of specific movement directions by neurons in the primary motor
1007 cortex." PLoS Biol **2**(2): E45.
- 1008 Pearson, T. S., J. W. Krakauer, et al. (2010). "Learning not to generalize: modular
1009 adaptation of visuomotor gain." J Neurophysiol **103**(6): 2938-2952.
- 1010 Pine, Z. M., J. W. Krakauer, et al. (1996). "Learning of scaling factors and reference
1011 axes for reaching movements." Neuroreport **7**(14): 2357-2361.

- 1012 Poggio, T. and E. Bizzi (2004). "Generalization in vision and motor control." *Nature*
1013 **431**(7010): 768-774.
- 1014 Pouget, A. and L. H. Snyder (2000). "Computational approaches to sensorimotor
1015 transformations." *Nat Neurosci* **3 Suppl**: 1192-1198.
- 1016 Rapp, K. and H. Heuer (2011). "Active error corrections enhance adaptation to a
1017 visuomotor rotation." *Exp Brain Res* **211**(1): 97-108.
- 1018 Savitzky, A. G., M.J.E. (1964). "Smoothing and Differentiation of Data by Simplified
1019 Least Squares Procedures." *Analytical Chemistry* **36**(8): 1627-1639.
- 1020 Shabbott, B. A. and R. L. Sainburg (2010). "Learning a visuomotor rotation:
1021 simultaneous visual and proprioceptive information is crucial for visuomotor
1022 remapping." *Exp Brain Res* **203**(1): 75-87.
- 1023 Smith, M. A., J. Brandt, et al. (2000). "Motor disorder in Huntington's disease begins as
1024 a dysfunction in error feedback control." *Nature* **403**(6769): 544-549.
- 1025 Tanaka, H., T. J. Sejnowski, et al. (2009). "Adaptation to visuomotor rotation through
1026 interaction between posterior parietal and motor cortical areas." *J Neurophysiol*
1027 **102**(5): 2921-2932.
- 1028 Taylor, D. M., S. I. Tillery, et al. (2002). "Direct cortical control of 3D neuroprosthetic
1029 devices." *Science* **296**(5574): 1829-1832.
- 1030 Thoroughman, K. A. and R. Shadmehr (2000). "Learning of action through adaptive
1031 combination of motor primitives." *Nature* **407**(6805): 742-747.
- 1032 Thoroughman, K. A. and J. A. Taylor (2005). "Rapid reshaping of human motor
1033 generalization." *J Neurosci* **25**(39): 8948-8953.
- 1034 Tseng, Y. W., J. Diedrichsen, et al. (2007). "Sensory prediction errors drive cerebellum-
1035 dependent adaptation of reaching." *J Neurophysiol* **98**(1): 54-62.
- 1036 Vindras, P. and P. Viviani (2002). "Altering the visuomotor gain. Evidence that motor
1037 plans deal with vector quantities." *Exp Brain Res* **147**(3): 280-295.
- 1038

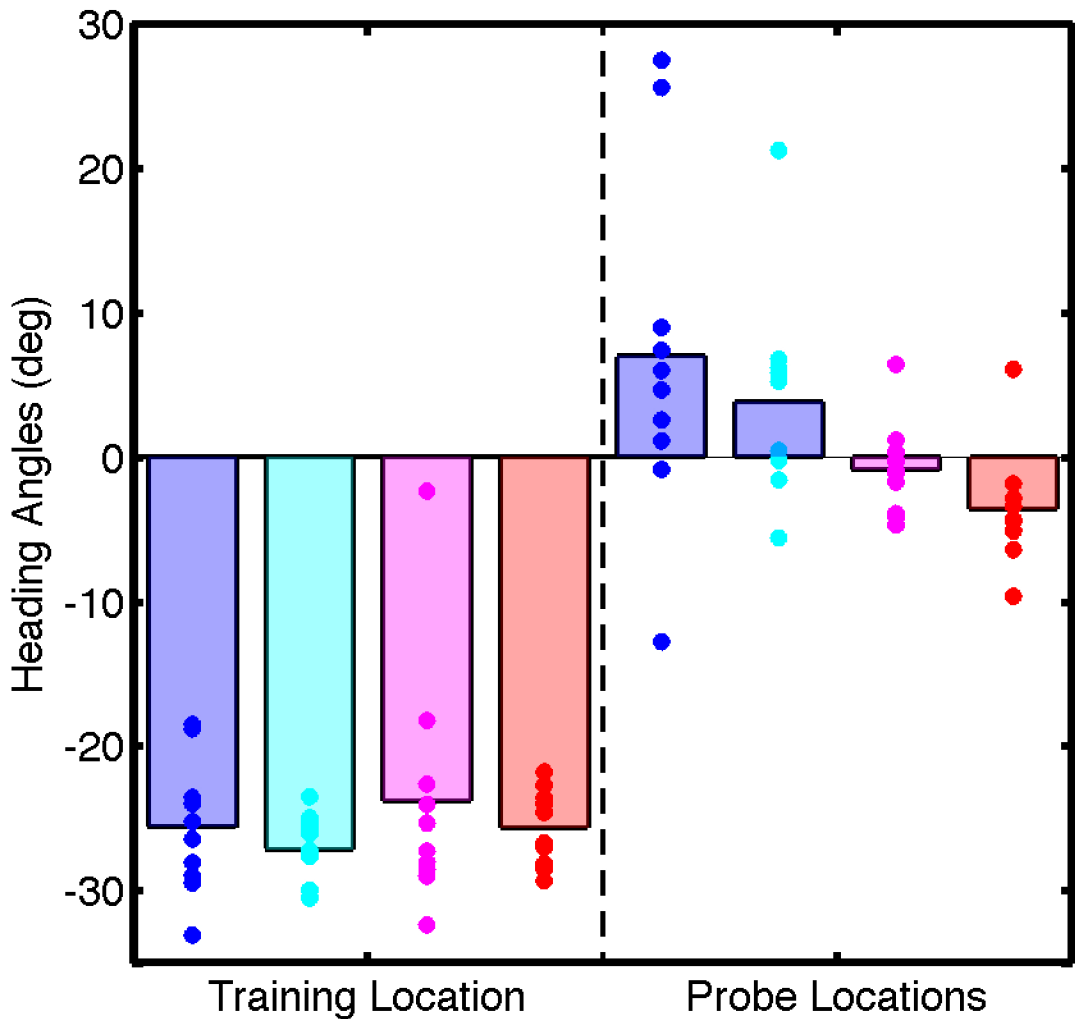


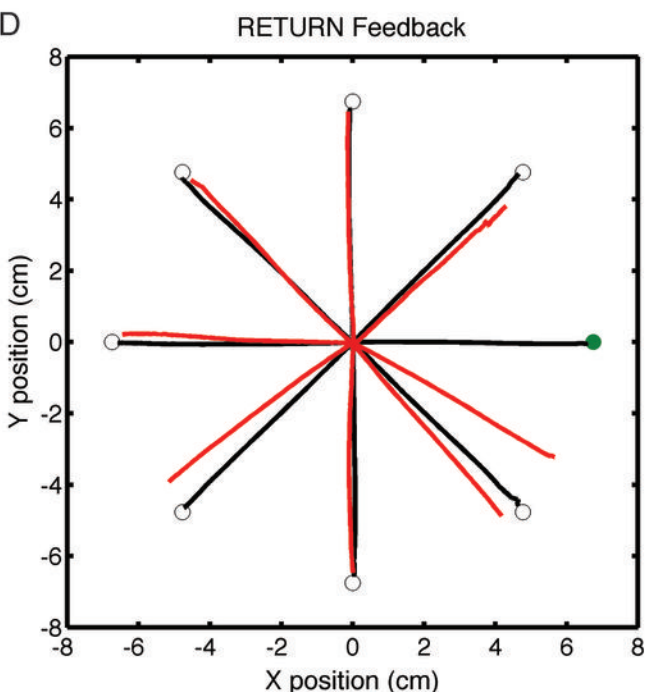
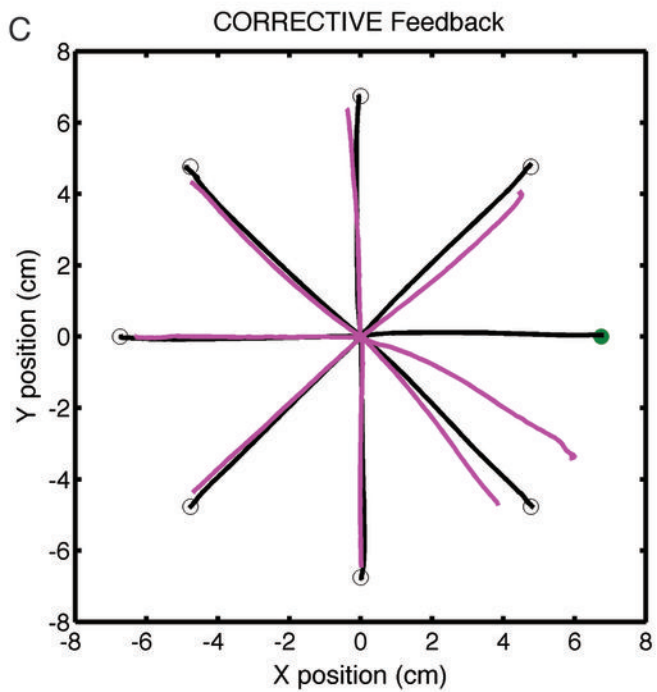
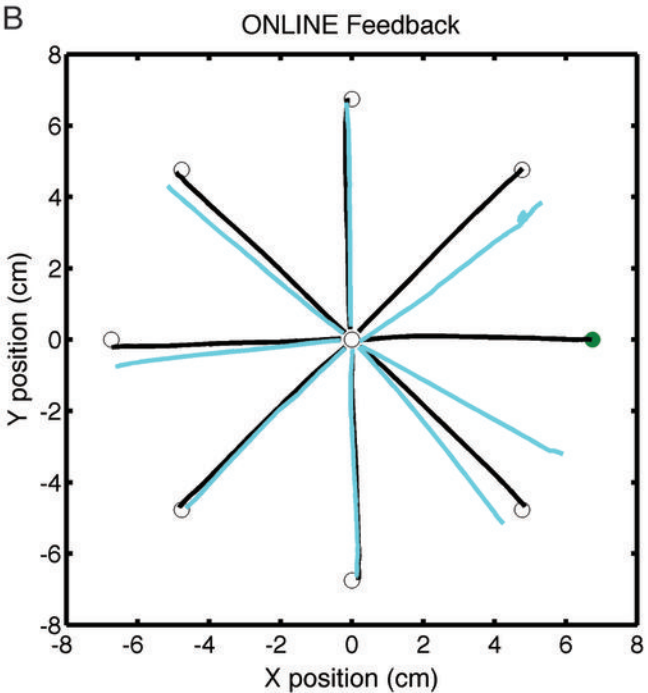
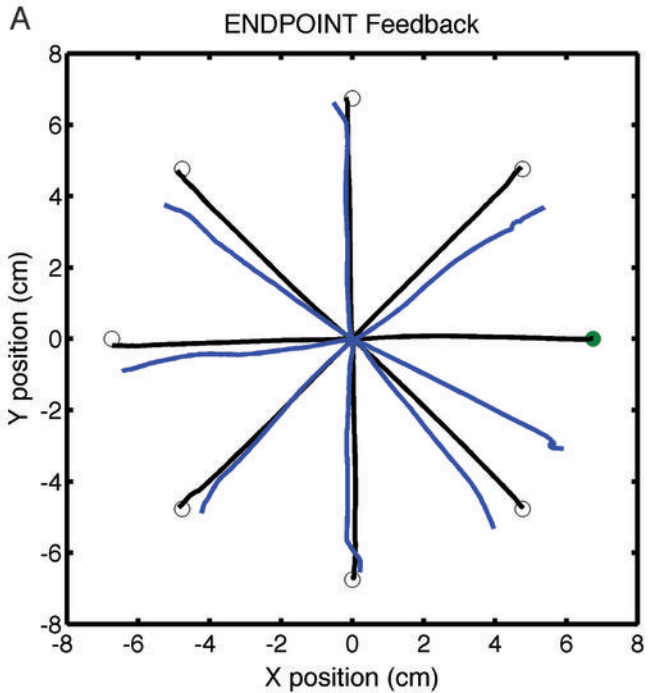
Training Time Course





Test Block Generalization





Simulated Training Time Course

